Quantifying Mechanical Properties of Liver Tissue for Specimen-specific Finite-element Models

Yuan-Chiao Lu, Andrew R. Kemper, Costin D. Untaroiu

Virginia Tech
Wake Forest University
School of Biomedical Engineering and Sciences

Introduction

Human finite element (FE) models play an important role in understanding the injury mechanism during a crash and designing advanced restraint systems. However, the accuracy of FE models depends not only on geometrical properties, but also on assigned material models. While various experimental tissue tests of abdominal organs have been conducted, the specimen-specific FE modeling of abdominal organs has rarely been attempted in previous studies and the material models for FE simulation of abdominal tissues are still largely unknown [1-3]. Therefore, the goal of this study was to conduct the tensile testing on bovine abdominal tissue and then to identify material models using FE specific models and optimization techniques. The methodology developed in this study will be further applied to build material models of human tissues.

Test Procedure

10 Fresh Bovine Livers

Coupon Specimens

Strain Rate 1: 0.01 s^{-1} | Strain Rate 2: 0.1 s^{-1} | Strain Rate 3: 1.0 s^{-1}

Experimental Tensile Testing

Finite-Element Models and Optimization

Finite-Element Material Models for Abdominal Tissues

Methods

- Uniaxial tensile tests were performed on the parenchyma of 10 fresh bovine livers obtained from Animal Technologies (Tyler, Texas, USA).
- Coupon specimens (thickness: 5 mm) were cut from the livers with a custom blade assembly (Fig. 1-3) and tested within 36 hours after slaughter.
- Each liver was divided into three categories which were tested until failure at the following strain rates: 0.01 s^{-1}, 0.1 s^{-1}, and 1.0 s^{-1}.
- A uniaxial load cell was mounted between the linear actuator and the upper clamp (Fig. 4).
- Each specimen was stretched at the two ends, and the time histories of force and displacement were recorded during testing.
- Specimens were immersed in a bath of Dulbecco's Modified Eagle Medium (DMEM) to maintain specimen hydration until test at 98^{0}F.

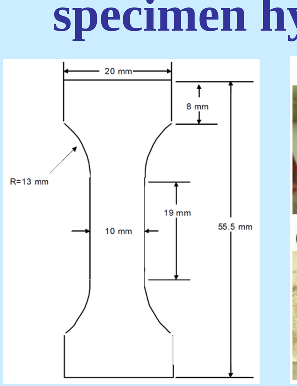

Figure 1. Coupon specimen size.

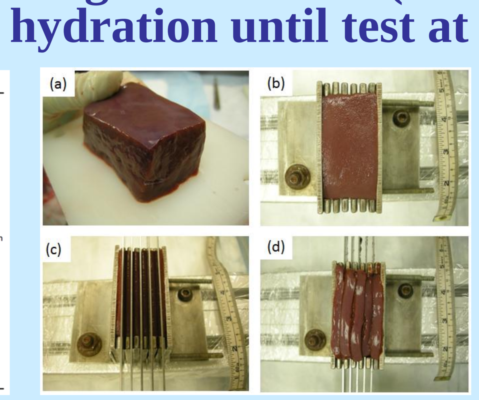

Figure 2. Specimen slicing methodology.

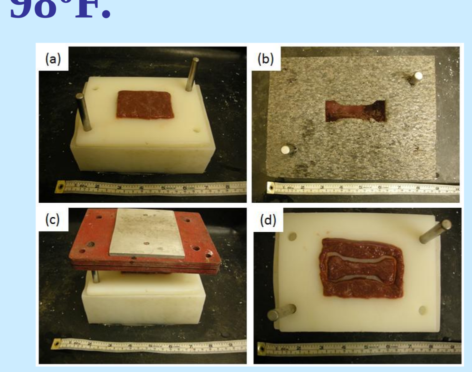

Figure 3. Specimen stamping Methodology.

Data Analysis

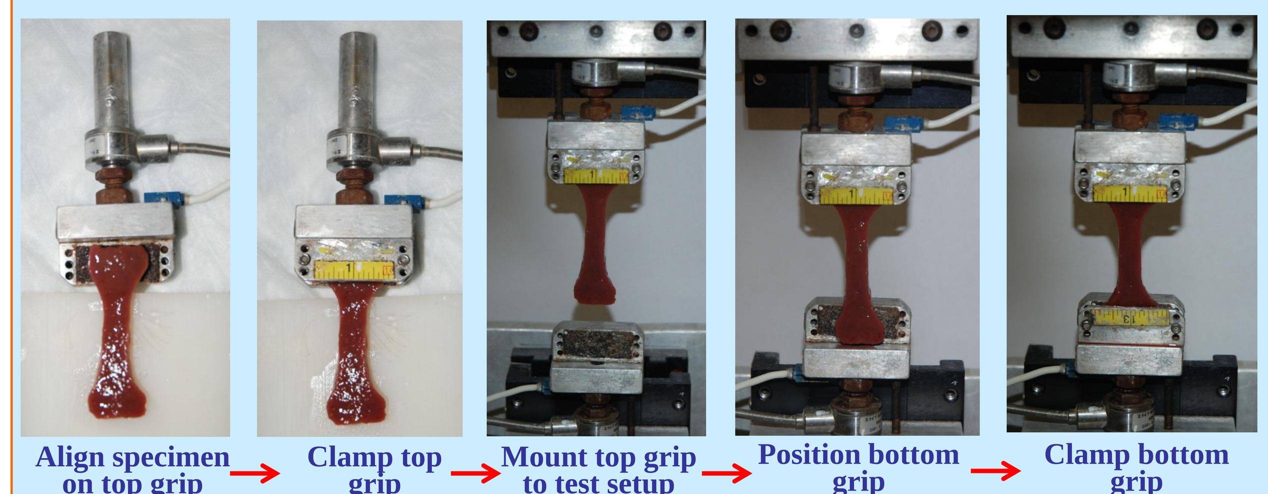

Figure 4. Specimen mounting methodology.

- Optical markers were tracked throughout the duration of the test using motion analysis software (TEMA, Linkoping, Sweden).

- Stretch Ratio $\lambda = \frac{L_n}{L_0}$
  - L_0: the original distance between the optical markers
  - L_n: the instantaneous distance between the optical markers.
- Green-Lagrange Strain $\boldsymbol{\varepsilon} = \frac{1}{2}(\lambda^2 - 1)$
- Inertially Compensated Force $F_{IC} = F - a * m_{eff}$
  - F: measured force
  - a: grip acceleration
  - m_{eff}: effective mass
- 2nd Piola-Kirchhoff Stress $S = \frac{F_{IC}}{\lambda * A_0}$
  - A_0: initial cross-sectional area at the tear site
- Comparison of failure stress and failure stain
  - Two-sample unpaired t-test (assuming unequal variance)

Results

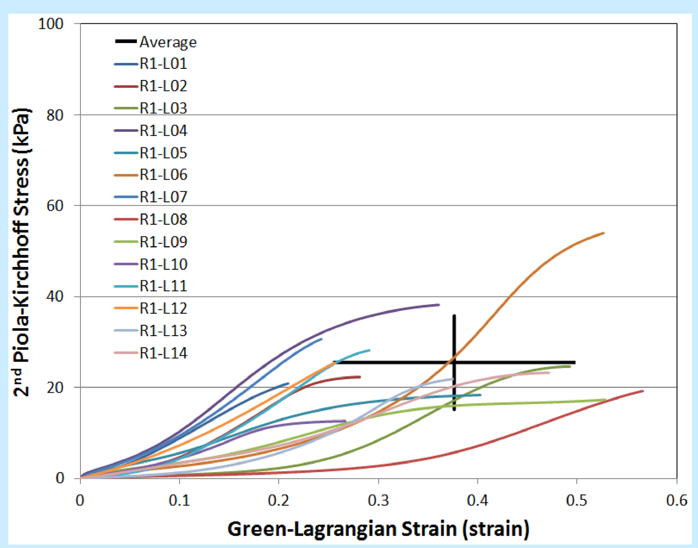

(a) Strain Rate: 0.01 s^{-1}

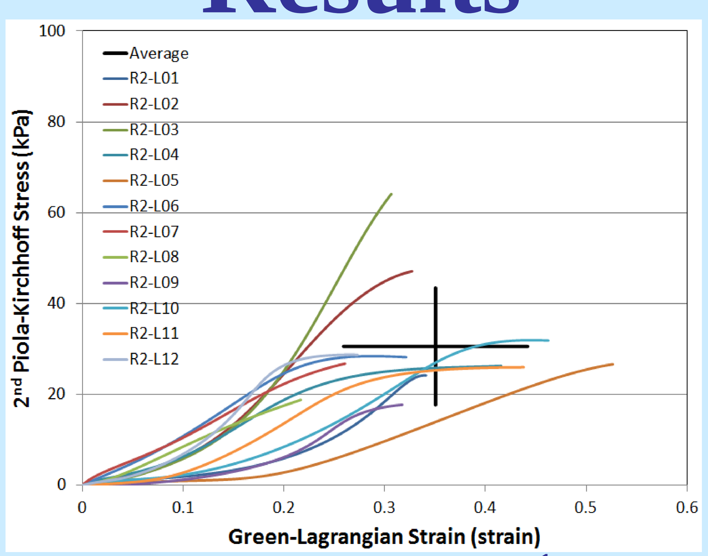

(b) Strain Rate: 0.1 s^{-1}

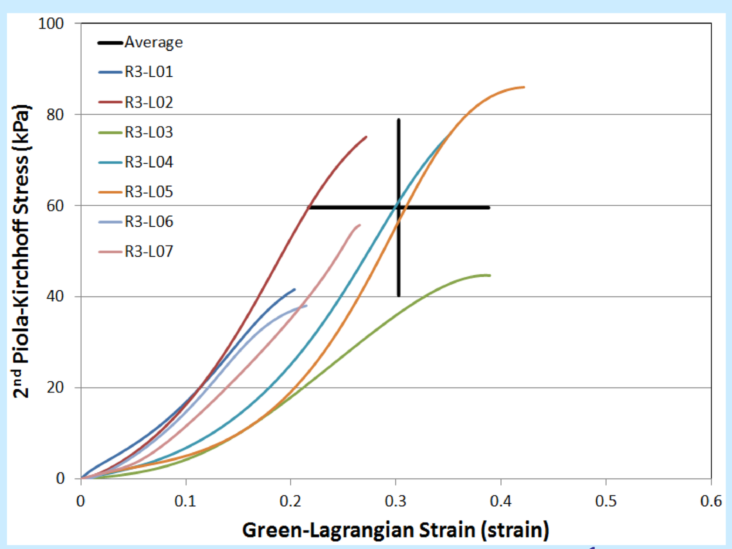

(c) Strain Rate: 1.0 s^{-1}

Figure 5. Second Piola-Kirchhoff stress vs. Green-Lagrangian strain curves of bovine liver tensile testing by loading rate.

Rate	#of Specimens	Desired Strain Rate (s^{-1})	Average Strain Rate (s^{-1})	Average Failure Strain	Average Failure Stress (kPa)
Rate 1	14	0.01	0.007 (±0.001)	0.376 (±0.122)	25.498 (±10.304)
Rate 2	12	0.1	0.071 (±0.007)	0.350 (±0.091)	30.553 (±12.873)
Rate 3	7	1.0	0.679 (±0.092)	0.303 (±0.086)	59.599 (±19.257)

Table 1. Averages and standard deviations of measured strain rate, failure strain and failure stress by loading rate.

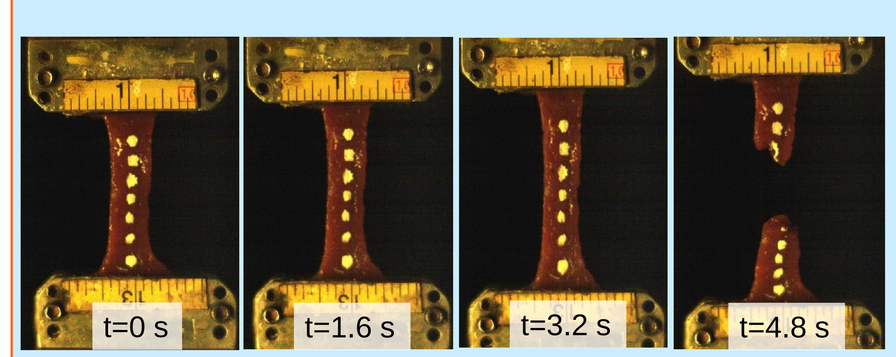

Figure 6. High-speed video stills of a typical uniaxial tensile test (Rate 2).

Rate	Data Acquisition (kHz)	Video (Hz)
Rate 1	0.2	20
Rate 2	2.0	70
Rate 3	20.0	500

Table 2. Data acquisition and video sampling rates by loading rate.

Comparison	Failure Strain p-value	Failure Stress p-value
Rate 1 vs. Rate 2	0.544	0.287
Rate 1 vs. Rate 3	0.127	**0.003**
Rate 2 vs. Rate 3	0.271	**0.006**

Table 3. Statistical comparison between rates. Bold: p-value<0.05.

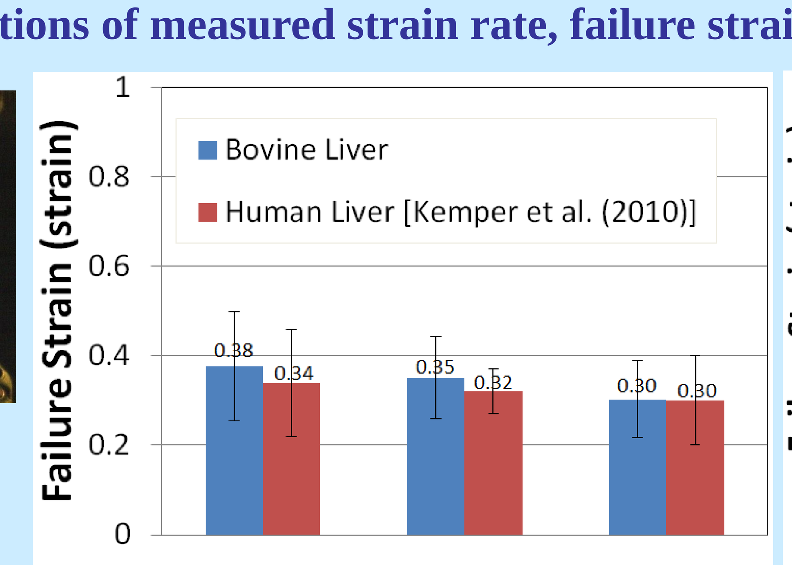

Figure 7. Comparison of tensile failure strain between bovine and human livers.

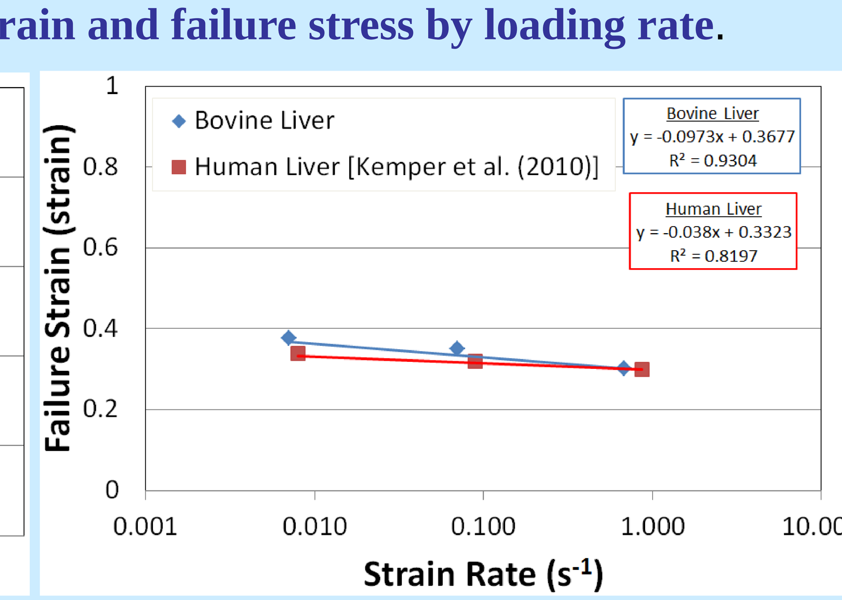

Figure 9. Failure strain vs. strain rate.

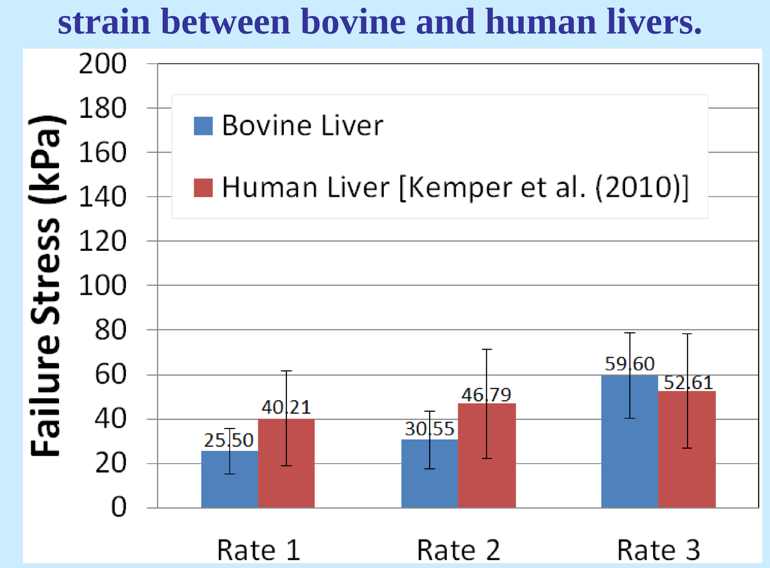

Figure 8. Comparison of tensile failure stress between bovine and human livers.

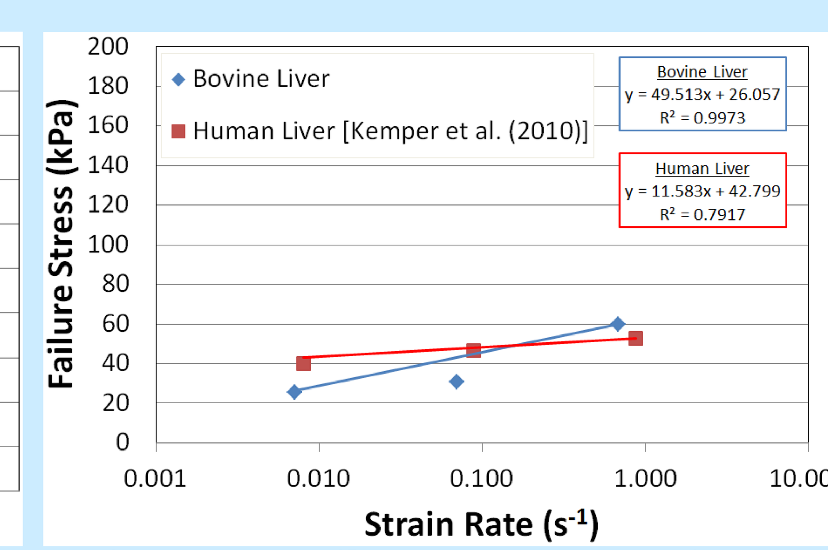

Figure 10. Failure stress vs. strain rate.

Discussion

- The current study quantifies the material response of fresh bovine liver parenchyma in tensile loading at various loading rates.
- The data from this study shows that the response of bovine liver parenchyma is non-linear and visco-elasticity in tensile loading.
- With increased loading rate, the failure stress significantly increased while the failure strain does not significantly decrease.
- The rate dependence of liver parenchyma should be taken into account when developing material models or injury thresholds.

Future Work

- The initial geometries of specimens were recorded using a FARO Laser Scanner (Beringen, Switzerland) and then used to develop the specimen-specific FE models (Fig. 11a,b).
- Parameter identification of material models for abdominal organs which use present reported test data and optimization techniques are currently ongoing [4,5].
- Several visco-hyperelastic material models were assigned to the specimens, and the tension tests were simulated in LS-DYNA software (Fig. 11c).
- The square root error between the time histories of force recorded in testing and simulations were defined as objective function and heuristic optimization algorithms (e.g. genetic algorithm) were used to identify the values of material coefficients.

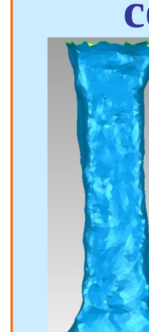

(a) Raw FARO scan data of a typical coupon specimen.

(b) Smoothed NURBS surface.

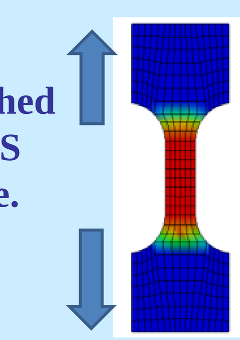

(c) The stress distribution in a specimen model during a preliminary test simulation.

Figure 11. Specimen-specific FE Models.

- It is believed that the methodology developed will be extended to human organs in the future to develop more accurate material models of abdominal organs, which consequently will result in more accurate FE human models.

Reference

[1] Kemper, A.R., Santago, A.C., Stitzel, J.D., Sparks, J.L., Duma, S.M., 2012. Biomechanical response of human spleen in tensile loading. Journal of Biomechanics 45(2), 348-355.

[2] Kemper, A.R., Santago, A.C., Stitzel, J.D., Sparks, J.L., Duma, S.M., 2010. Biomechanical response of human liver in tensile loading. Annals of Advances in Automotive Medicine 50, 15-26.

[3] Snedeker, J.G., Niederer, P., Schmidlin, F.R., Farshad, M., Demetropoulos, C.K., Lee, J.B., Yang, K.H., 2005. Strain-rate dependent material properties of the porcine and human kidney capsule. Journal of Biomechanics 38(5), 1011-1121.

[4] Raghunathan, S., Evans, D., Sparks, J.L., 2010. Poroviscoelastic modeling of liver biomechanical response in unconfined compression. Annals of Biomedical Engineering 38(5), 1789-1800.

[5] Hu, J., Klinich, K.D., Miller, C.S., Nazmi, G., Pearlman, M.D., Schneider, L.W., Rupp, J.D., 2009. Quantifying dynamic mechanical properties of human placenta tissue using optimization techniques with specimen-specific finite-element models. Journal of Biomechanics 42(15), 2528-2534.

Center for Injury Biomechanics

Yuan-Chiao Lu
Center for Injury Biomechanics Crash Sled Lab
Suite 1200, VCOM II Building, 2280 Kraft Drive, Blacksburg, VA 24060
YCLU@vt.edu